

Supplementary Information

Effect of Bulky Substituent on the Self-assembly and Mixing Behavior of Arylene Ethynylene Macrocycles at the Solid-Liquid Interface

Lirong Xu¹, Liu Yang¹, Lili Cao¹, Tian Li², Shusen Chen², Dahui Zhao^{2*}, Shengbin Lei^{1*}, Jun Ma¹

1. Large scale STM images of the assembly of AEM-B, AEM-N and AEM-A
2. High resolution STM images of AEM-B+AEM-N composite structure
3. STM images of AEM-B+AEM-A composite structure
4. Optimized conformation of AEMs
5. Characterization of AEMs

1. Large scale STM images of the assembly of AEM-B, AEM-N and AEM-A

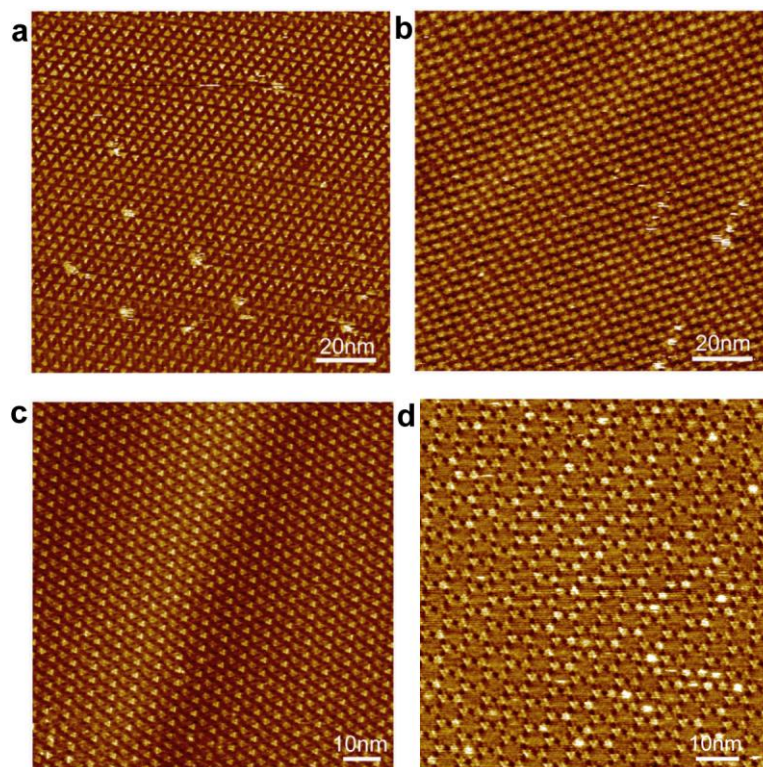


Figure S1. Large-scale STM images of AEM-B at the TCB/HOPG interface. (a) 5.33×10^{-4} mol/L, $I_{\text{set}} = 8$ pA, $V_{\text{set}} = 1.0$ V. (b) 5.33×10^{-4} mol/L, $I_{\text{set}} = 8$ pA, $V_{\text{set}} = 1.0$ V. (c)

5.33×10^{-5} mol/L, $I_{\text{set}} = 8$ pA, $V_{\text{set}} = 1.0$ V. (d) 5.33×10^{-7} mol/L, $I_{\text{set}} = 109$ pA, $V_{\text{set}} = 1.0$ V. (a) and (b) both show the coexistence of linear A and linear B structures, where in (a) linear A is dominant and in (b) linear B is dominant. (c) and (d) are the linear C and honeycomb structure, respectively.

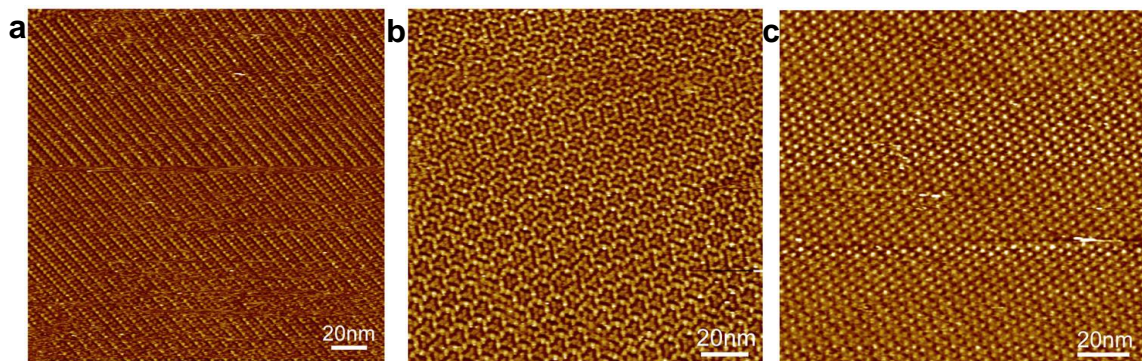


Figure S2. Large-scale STM images of linear, flower and filled honeycomb structure of AEM-N at the TCB/HOPG interface. (a) Linear structure, 4.90×10^{-4} mol/L, $I_{\text{set}} = 5$ pA, $V_{\text{set}} = 1.2$ V. (b) Flower structure, 4.90×10^{-4} mol/L, $I_{\text{set}} = 5$ pA, $V_{\text{set}} = 1.2$ V. (c) Filled honeycomb structure, 4.90×10^{-6} mol/L, $I_{\text{set}} = 5$ pA, $V_{\text{set}} = 1.2$ V.

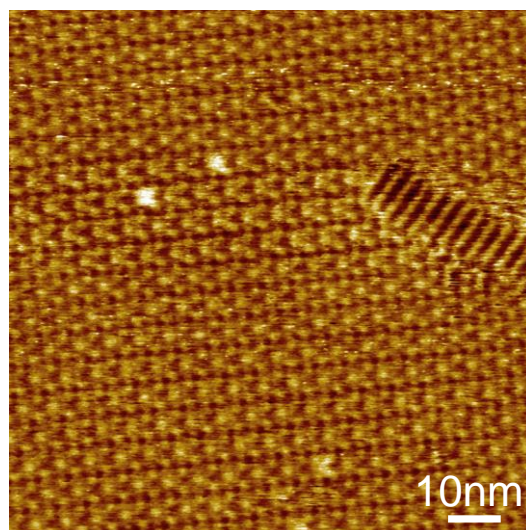


Figure S3. Large-scale STM image of AEM-A. 4.53×10^{-4} mol/L, $I_{\text{set}} = 5$ pA, $V_{\text{set}} = 0.8$ V.

2. High resolution STM images of AEM-B+AEM-N composite structure

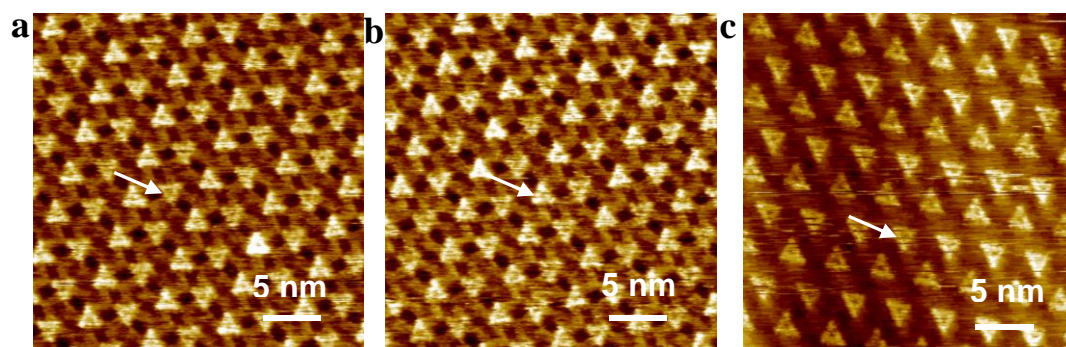


Figure S4. (a-c) High resolution STM images of AEM-B and AEM-N composite structures at the TCB/HOPG interface. AEM-B: 3.55×10^{-6} mol/L, AEM-N: 1.63×10^{-6} mol/L, AEM-B: AEM-N= 2.18, $I_{\text{set}}= 8$ pA, $V_{\text{set}}= 1.2$ V. The white arrows mark one of AEM-B molecule in the framework.

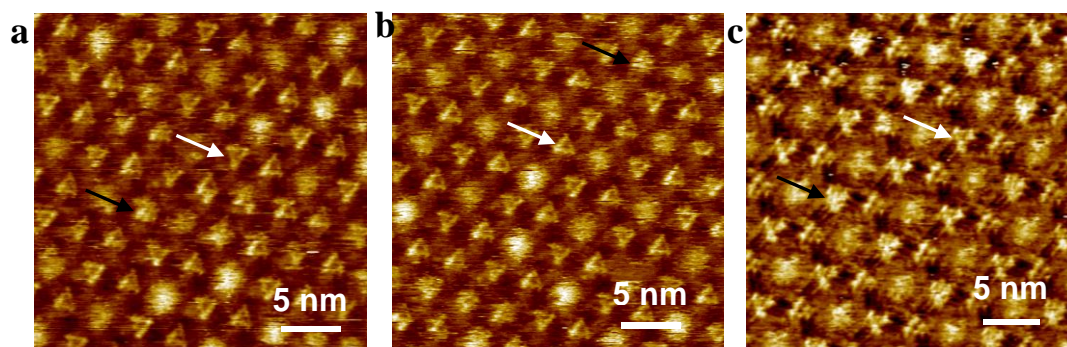


Figure S5. (a-c) High resolution STM images of AEM-B and AEM-N composite structures at the TCB/HOPG interface. AEM-B: 2.67×10^{-6} mol/L, AEM-N: 2.45×10^{-6} mol/L, AEM-B: AEM-N= 1.09, $I_{\text{set}}= 8$ pA, $V_{\text{set}}= 1.2$ V. The white and black arrows mark one of AEM-B and AEM-N molecule in the hybrid network, respectively.

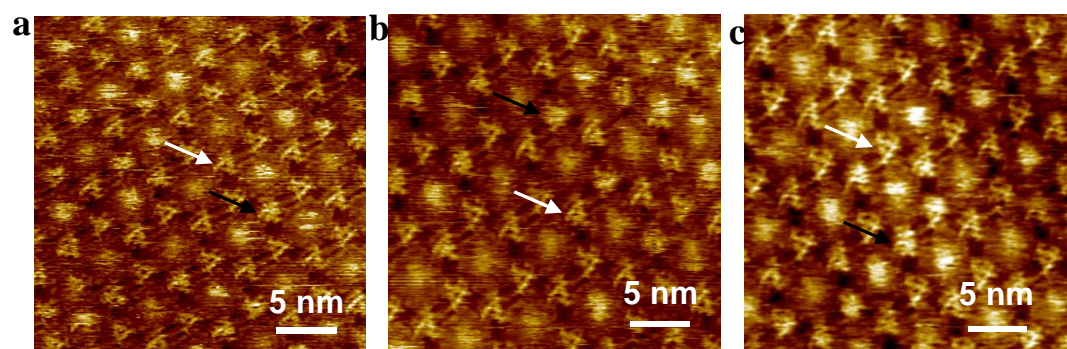


Figure S6. (a-c) High resolution STM images of AEM-B and AEM-N composite structures at the TCB/HOPG interface. AEM-B: 1.78×10^{-6} mol/L, AEM-N: 3.27×10^{-6} mol/L, AEM-B: AEM-N= 0.54, $I_{\text{set}}= 9$ pA, $V_{\text{set}}= 0.9$ V. The white and black arrows mark one of AEM-B and AEM-N molecule in the hybrid network, respectively.

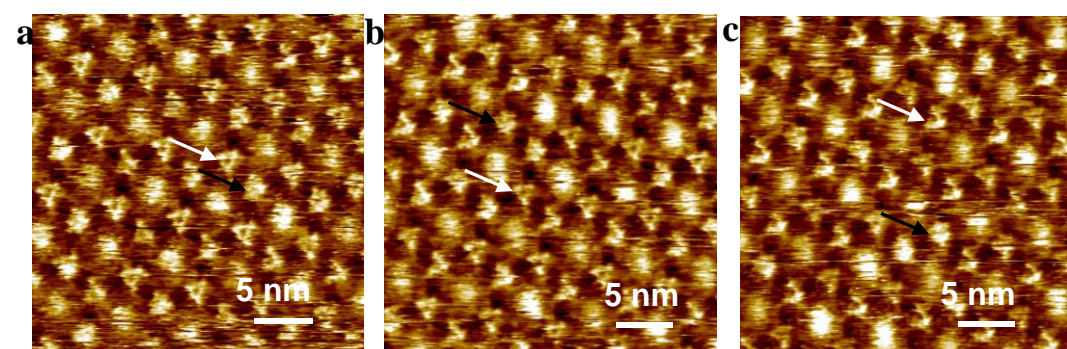


Figure S7. (a-c) High resolution STM images of AEM-B and AEM-N composite structures at the TCB/HOPG interface. AEM-B: 1.33×10^{-6} mol/L, AEM-N: 3.67×10^{-6} mol/L, AEM-B: AEM-N = 0.36, $I_{\text{set}} = 6$ pA, $V_{\text{set}} = 1.2$ V. The white and black arrows mark one of AEM-B and AEM-N molecule in the hybrid network, respectively.

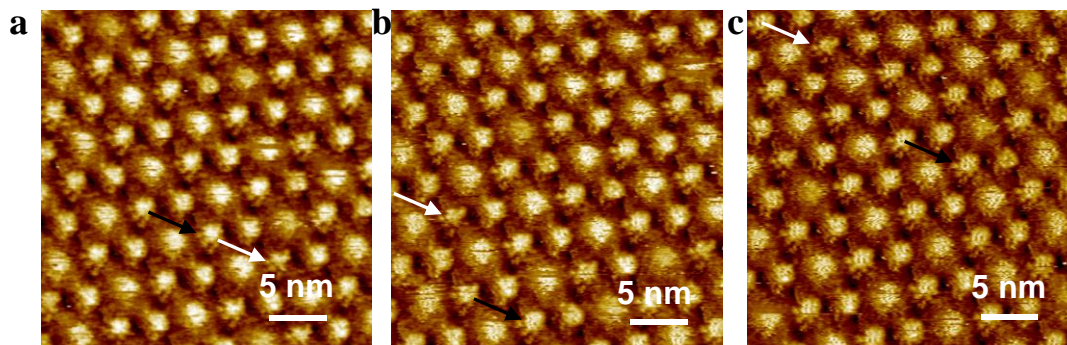


Figure S8. (a-c) High resolution STM images of AEM-B and AEM-N composite structures at the TCB/HOPG interface. AEM-B: 1.07×10^{-6} mol/L, AEM-N: 3.92×10^{-6} mol/L, AEM-B: AEM-N = 0.27, $I_{\text{set}} = 70$ pA, $V_{\text{set}} = 0.8$ V. The white and black arrows mark one of AEM-B and AEM-N molecule in the hybrid network, respectively.

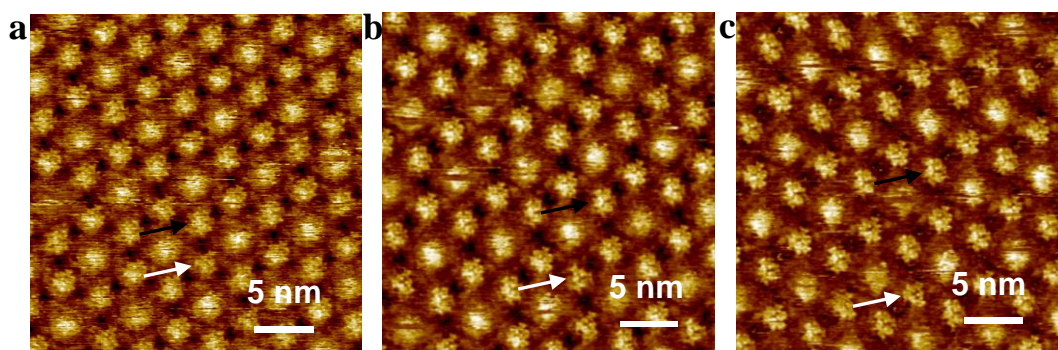


Figure S9. (a-c) High resolution STM images of AEM-B and AEM-N composite structures at the TCB/HOPG interface. AEM-B: 5.92×10^{-7} mol/L, AEM-N: 4.36×10^{-6} mol/L, AEM-B: AEM-N = 0.14, $I_{\text{set}} = 50$ pA, $V_{\text{set}} = 1.0$ V. The white and black arrows mark one of AEM-B and AEM-N molecule in the hybrid network, respectively.

3. STM images of AEM-B+AEM-A composite structure

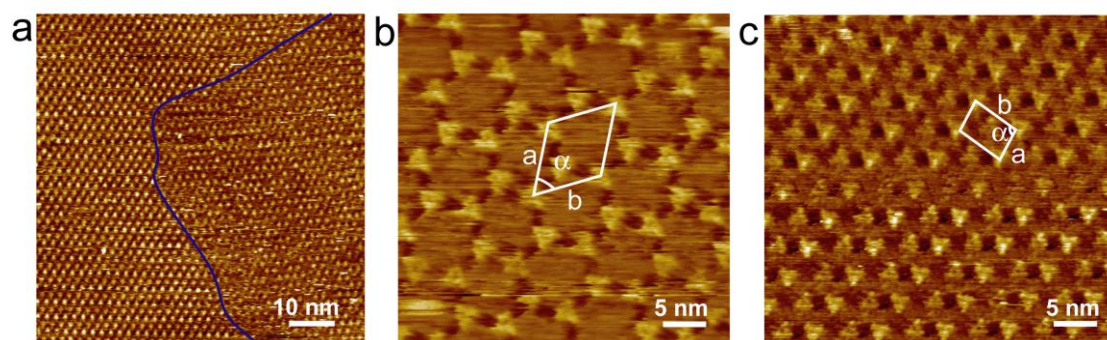


Figure S10. STM images of AEM-B and AEM-A composite structures. (a)

Large-scale STM image of AEM-B and AEM-A composite structure at the TCB/HOPG interface. The blue curve separates a honeycomb and a linear domain; (b) and (c): High resolution STM image of honeycomb and linear structure. A unit cell is indicated in white for each structure. AEM-B: 1.33×10^{-6} mol/L, AEM-A: 3.40×10^{-6} mol/L, AEM-B: AEM-A = 0.39, $I_{\text{set}} = 8$ pA, $V_{\text{set}} = 1.2$ V.

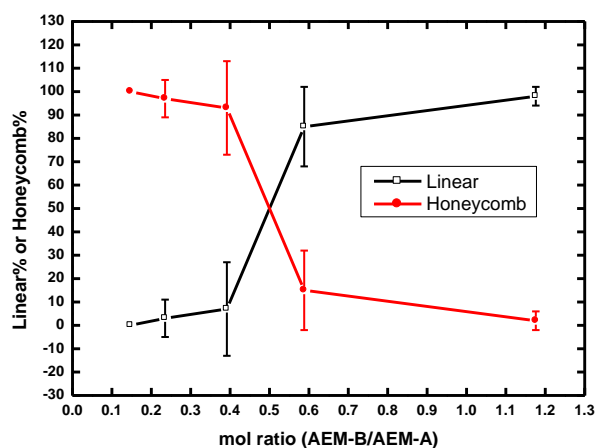


Figure S11. Dependence of surface coverage of linear and honeycomb structure of AEM-B on the mol ratio of AEM-B/ AEM-A in solution. Please note that the large error is caused by the big size of the domains which frequently exceed the scanning area of the images used for statistics.

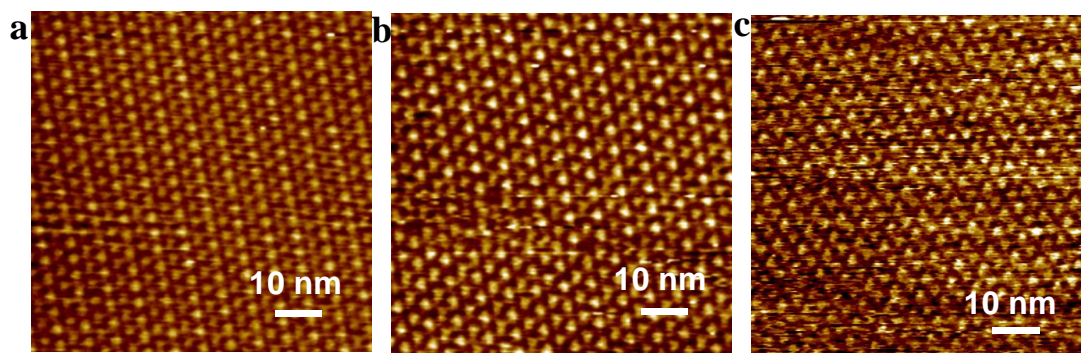


Figure S12. (a-c) Large scale STM images of AEM-B and AEM-A composite structures at the TCB/HOPG interface. AEM-B: 2.67×10^{-6} mol/L, AEM-A: 2.27×10^{-6} mol/L, AEM-B : AEM-A = 1.18, $I_{\text{set}} = 8$ pA, $V_{\text{set}} = 1.2$ V.

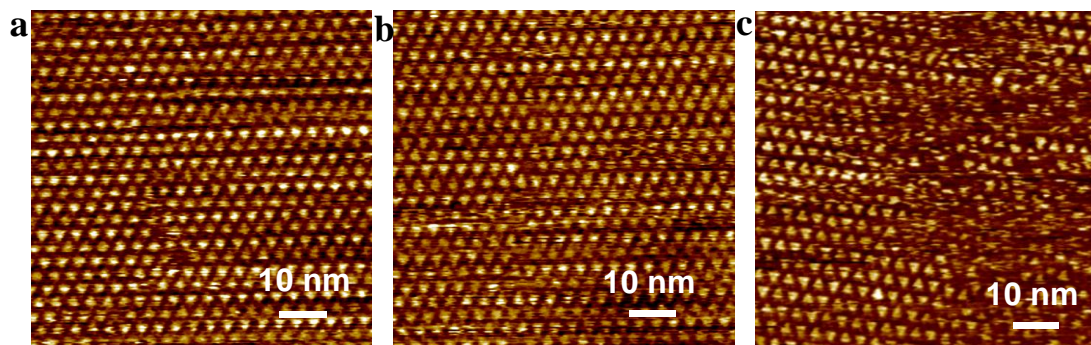


Figure S13. (a-c) Large scale STM images of AEM-B and AEM-A composite structures at the TCB/HOPG interface. AEM-B: 1.78×10^{-6} mol/L, AEM-A: 3.02×10^{-6} mol/L, AEM-B: AEM-A = 0.59, $I_{\text{set}} = 8$ pA, $V_{\text{set}} = 1.5$ V.

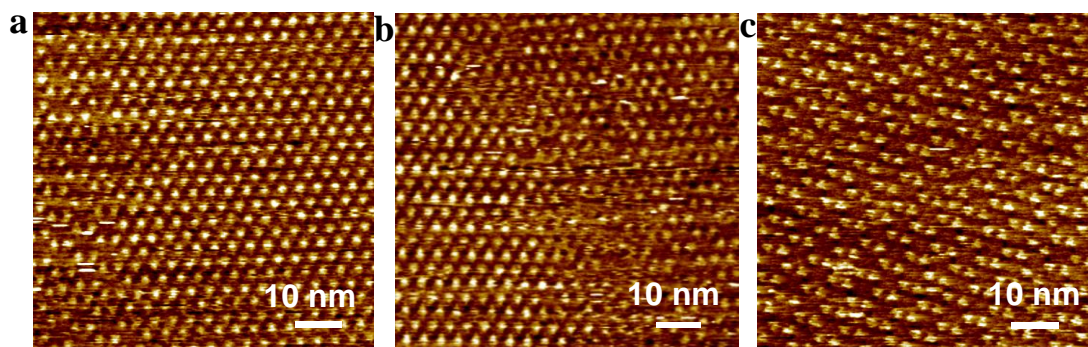


Figure S14. (a-c) Large scale STM images of AEM-B and AEM-A composite structures at the TCB/HOPG interface. AEM-B: 1.33×10^{-6} mol/L, AEM-A: 3.40×10^{-6} mol/L, AEM-B: AEM-A = 0.39, $I_{\text{set}} = 40$ pA, $V_{\text{set}} = 1.2$ V.

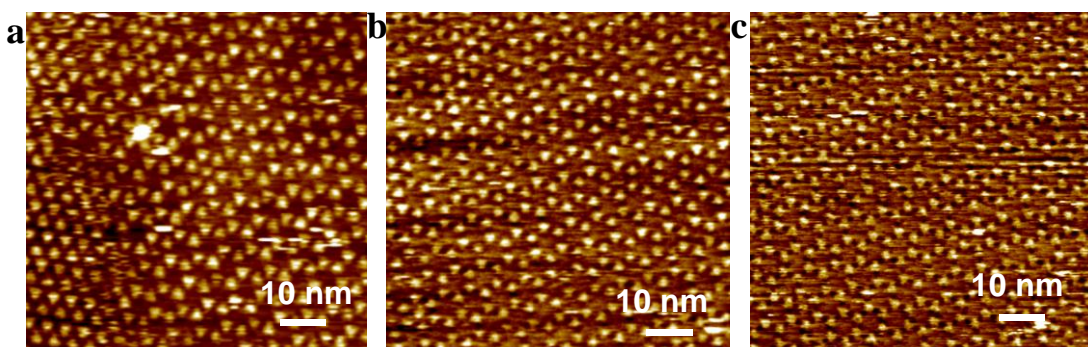


Figure S15. (a-c) Large scale STM images of AEM-B and AEM-A composite structures at the TCB/HOPG interface. 8.89×10^{-7} mol/L, AEM-A: 3.78×10^{-6} mol/L, AEM-B: AEM-A = 0.24, $I_{\text{set}} = 8$ pA, $V_{\text{set}} = 1.2$ V.

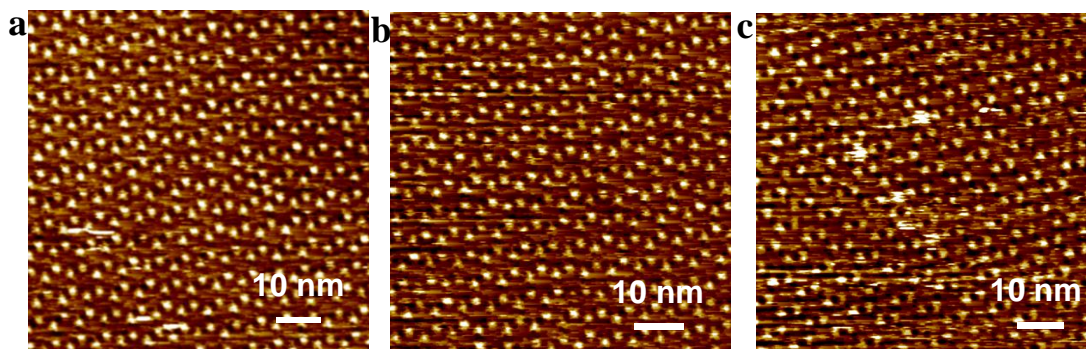


Figure S16. (a-c) Large scale STM images of AEM-B and AEM-A composite structures at the TCB/HOPG interface. 5.92×10^{-7} mol/L, AEM-A: 4.03×10^{-6} mol/L,

AEM-B: AEM-A= 0.15, $I_{\text{set}}= 4 \text{ pA}$, $V_{\text{set}}= 1.2 \text{ V}$.

4. Optimized conformation of AEMs

The conformation of AEMs were optimized using molecular mechanics with MM+ force field provided by Hyperchem software. The optimization was performed in Voccum on a single layer graphene as substrate. For simplicity the side chains are replaced with methoxy groups. After adsorption on graphene, AEM-B and AEM-N both adapt planar conformation with the phenylene ethynylene side slightly bended. While AEM-A can not adapt planar conformation because of the steric repulsion between the bulky anthrylene groups. Significant distortion can be clearly observed from the side view on two of the three anthrylene groups.

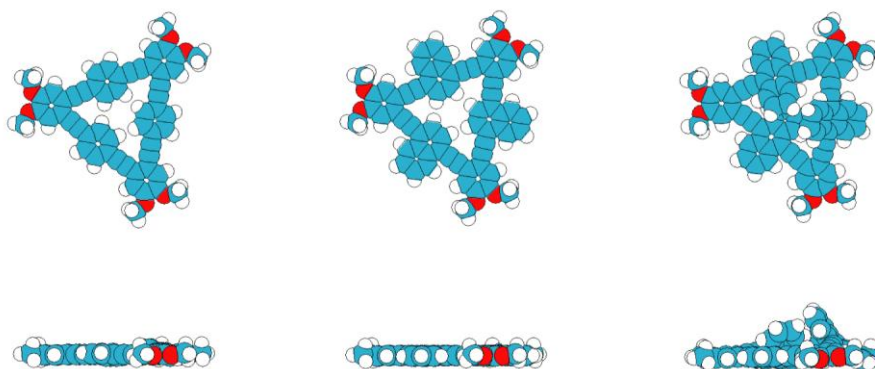


Figure S17. top and side view of optimized conformations of AEM-B, AEM-N and AEM-A. The graphite substrate was omitted for clarity.

5. Characterization of AEMs

AEM-B

$^1\text{H NMR}$ (300 MHz, CDCl_3): δ 7.56 (12H, s), 7.03 (6H, s), 4.04 (12H, t, $J = 6.5$ Hz), 1.85 (12H, m), 1.48 (12H, m), 1.2-1.4 (96H, m), 0.89 (18H, t, $J = 6.4$ Hz). $^{13}\text{C NMR}$ (75 MHz, CDCl_3): δ 149.2, 131.2, 123.2, 118.5, 115.6, 92.0, 90.7, 69.1, 31.9, 29.72, 29.68, 29.66, 29.43, 29.38, 29.1, 26.0, 22.7, 14.1. FT-IR (KBr): 2921, 2851, 1639, 1520, 1482, 1363, 1244, 1203, 1077, 824, 717 cm^{-1} . MALDI-TOF MS: Calcd. for $\text{C}_{120}\text{H}_{168}\text{O}_6$: 1705.3. Found: 1704.8 (M^+). Anal. Calcd. for $\text{C}_{120}\text{H}_{168}\text{O}_6$: C, 84.45; H, 9.92. Found: C, 84.55; H, 10.06.

AEM-N

$^1\text{H NMR}$ (400 MHz, CDCl_3): δ 8.46-8.43 (6H, m), 7.67 (6H, s), 7.20 (6H, s), 6.98-6.95 (6H, m), 4.14-4.10 (12H, t, $J = 6.6$ Hz), 1.91-1.88 (12H, m), 1.45-1.20 (108H, m), 0.89-0.86 (18H, m). $^{13}\text{C NMR}$ (75 MHz, CDCl_3): δ 149.5, 132.8, 129.8, 129.7, 127.0, 126.7, 121.4, 118.7, 116.0, 95.2, 90.3, 69.3, 31.9, 29.6, 29.4, 29.2,

26.0, 22.7, 14.1. MALDI-TOF MS: Calcd for C₁₃₂H₁₇₄O₆: 1855.3 (m/z, 70%), 1856.3 (m/z, 100%). Found: 1857.4 (m/z). Anal. Calcd. for C₁₃₂H₁₇₄O₆: C, 85.38; H, 9.45. Found: C, 85.08; H, 9.36.

AEM-A

¹H NMR(400 MHz, CDCl₃): δ 8.57-8.54 (12H, m), 7.33 (6H, s), 6.76-6.73 (12H, m), 4.19-4.16 (12H, t, J= 6.4 Hz), 1.95-1.92 (12H, m), 1.55-1.27 (108H, m), 0.89-0.86 (18H, m). ¹³C NMR (75 MHz, CDCl₃): δ 149.6, 131.9, 127.1, 126.4, 119.0, 118.2, 116.0, 101.2, 89.2, 69.4, 43.6, 31.9, 29.72, 29.66, 29.44, 29.38, 29.2, 26.0, 22.7, 14.1. MALDI-TOF MS: Calcd for C₁₄₄H₁₈₀O₆: 2005.4 (m/z, 63%), 2006.4 (m/z, 100%). Found: 2007.4 (m/z). Elem. Anal. Calcd. for C₁₄₄H₁₈₀O₆: C, 86.18; H, 9.04. Found: C, 86.29; H, 8.90.

References

1. Chen, S. S.; Yan, Q. F.; Li, T.; Zhao, D. H. Arylene Ethynylene Macrocycles with Intramolecular π - π Stacking. *Org. Lett.* **2010**, 12, 4784-4787.
2. Li, T.; Yue, K.; Yan, Q. F.; Huang, H. L.; Wu, H.; Zhu, N. B.; Zhao D. H. Triangular arylene ethynylene macrocycles: syntheses, optical, and thermotropic liquid crystalline properties. *Soft Matter*, **2012**, 8, 2405-2415.